Supporting Information for the article:

Proteostasis disturbances and endoplasmic reticulum stress contribute to polycystic liver disease: new therapeutic targets

Alvaro Santos-Laso,[1] Laura Izquierdo-Sanchez,[1,2] Pedro M. Rodrigues,[1] Bing Q. Huang,[3] Mikel Azkargorta,[2,4] Ainhoa Lapitz,[1] Patricia Munoz-Garrido,[1] Ander Arbelaiz,[1] Francisco J. Caballero,[1,5] Maite G. Fernandez-Barrena,[2,6] Raul Jimenez-Agüero,[1] Josepmaria Argemi,[6] Tomas Aragon,[6] Felix Elortza,[2,4] Marco Marzioni,[7] Joost P.H. Drenth,[8] Nicholas F. LaRusso,[3] Luis Bujanda,[1,2] Maria J. Perugorria,[1,2,9,§] and Jesus M. Banales[1,2,9,§]

[1]Department of Liver and Gastrointestinal Diseases, Biodonostia Research Institute – Donostia University Hospital –, University of the Basque Country (UPV/EHU), San Sebastian, Spain; [2]National Institute for the Study of Liver and Gastrointestinal Diseases (CIBERehd, Instituto de Salud Carlos III), Madrid, Spain; [3]Division of Gastroenterology and Hepatology, Mayo Clinic, Rochester, MN, USA; [4]Proteomics Platform, CIC bioGUNE, ProteoRed-ISCIII, Bizkaia Science and Technology Park, Derio, Spain; [5]Department of Organic Chemistry I, Center for Innovation in Advanced Chemistry (ORFEO-CINQA), University of the Basque Country (UPV/EHU), San Sebastian, Spain; [6]Division of Hepatology, CIMA-University of Navarra, Pamplona, Spain; [7]Department of Gastroenterology and Hepatology, Università Politecnica delle Marche, Ancona, Italy; [8]Department of Gastroenterology and Hepatology, Radboud University Medical Center, Nijmegen, The Netherlands; [9]IKERBASQUE, Basque Foundation for Science, Bilbao, Spain.

[§]Both authors share co-seniorship.

***Correspondence*:** Jesus M. Banales, PhD, Department of Liver and Gastrointestinal Diseases, Biodonostia Health Research Institute – Donostia University Hospital, Paseo del Dr. Begiristain s/n, E-20014, San Sebastian, Spain. e-mail: jesus.banales@biodonostia.org / Phone: +34 943006067; Fax: +34 943006250

or

Maria J. Perugorria, PhD, Department of Liver and Gastrointestinal Diseases, Biodonostia Health Research Institute – Donostia University Hospital, Paseo del Dr. Begiristain s/n, E-20014, San Sebastian, Spain. Email: matxus.perugorria@biodonostia.org / Phone: +34 943006125; Fax: +34 943006250

Table of content

Materials and methods

PLD animal model

8-weeks-old PCK male rats were divided in the following 4 groups: i) control (n=12), ii) 4-phenylbutyric acid sodium salt (4-PBA; Scandinavian formulas, PA, USA) (n=12), iii) tunicamycin (TM; Sigma, MO, USA) (n=12), and iv) dual 4-PBA & TM (n=12). Simultaneously, a wild-type (WT) group consisting of age- and gender-matched Sprague Dawley (SD) rats (n=12) were included in the study as healthy control animals. All the animals (i.e., SD and PCK rats) were purchased from Charles River Laboratories Inc. (Saint-Germain-sur-l'Arbresle, France).

Briefly, water supplemented with 4-PBA (100 mM) was given *ad libitum* for 20 weeks (i.e., 5 months), and the solution was replaced every 4 days. Water intake was periodically measured in control and 4-PBA treated groups, evidencing equal water consumption. On the other hand, TM (0.02 mg/kg/day) was injected intraperitoneally twice per week during 20 weeks.(1) Weight was measured once a week in order to adjust the TM dose. All animals were fed *ad libitum*. Approximately every 45 days, blood was collected from the rat tail in order to determine serum levels of alkaline phosphatase (ALP), aspartate aminotransferase (AST), alanine amino transferase (ALT), albumin, total protein, urea and creatinine. In addition, animal´s welfare was

monitored throughout the whole study. After this protocol, rats were sacrified and the hepatic and renal tissues were collected and, subsequently, analyzed at histological and molecular levels. Hematoxylin/eosin staining was used to visualize the architecture of the liver parenchyma and to calculate the relative cystic volume by multiplying the percentage of liver tissue occupied by cysts by the total volume (ml) of the corresponding liver tissue. The total cystic area was determined using the ImageJ software version 1.50 (NIH, Bethesda, MA, USA).

All the experimental procedures were approved by the Animal Experimentation Ethics Committees of both Biodonostia Health Research Institute (CEEA_17/009) and the Guipuzcoa Government (OH-17-19), and were used in conformity with the institution's guidelines for the use of laboratory animals.

Quantitative polymerase chain reaction (qPCR)

Total RNA was isolated from human and rat liver tissue samples, as well as from cells *in vitro*, using TRI-Reagent® (Sigma, MO, USA). Afterwards, total RNA isolated from cells and rat liver biopsies was reverse transcribed as previously described,(2) while *SuperScript Vilo cDNA Synthesis Kit* (Thermo Fisher Scientific, MA, USA) was used for human tissue samples, according to the manufacturer´s instructions. Finally, the expression (mRNA) of the UPR factors (i.e., *ATF6*, *IRE1α*, *PERK*, *GRP78, XBP1* and *CHOP*) and pro-inflammatory (i.e., *Il-6* and *Cxcl1*) and pro-fibrotic (i.e., *α-Sma, Col1a1* and *Ctgf*) genes (Supporting Table 2) were measured by qPCR in liver tissue and/or cells *in vitro,* using the *iQ™ SYBR® Green Supermix* (Bio-Rad) according to the manufacturer´s instructions. Primer sequences for each gene are included in Supporting Table 2. Gene expression was determined using the ΔCT method and *glyceraldehyde-3-phosphate dehydrogenase* (*GAPDH*) was used as internal housekeeping control. mRNA levels are represented as a percentage relative to the vehicle-treated control group.

Cell proliferation and death

Cell proliferation rate was determined by flow cytometry (Guava® easyCyte 8HT, Merck Millipore) in NHC, ADPKD and ADPLD cholangiocytes *in vitro*, in the presence or absence of 4-PBA (5 mM) for 48 h, using the CellTrace™ CFSE Cell Proliferation Kit (Invitrogen) as previously described.(3) Cell death (i.e., early and late apoptosis) assessment was performed by flow cytometry (Guava® easyCyte 8HT, Merck Millipore) in NHC, ADPKD and ADPLD cholangiocytes *in vitro*, in the presence or absence of TM (2.4 μM) and/or 4-PBA (5 mM) for 48 h, using a dual fluorescent staining method with fluorescein isotiocyanate (FITC) Annexin V (Biolegend, CA, USA) and TO-PRO®-3 (Thermo Fisher Scientific, MA, USA) fluorescence dyes. Briefly, 3-3.5x10^4 cells per well were seeded in a 24-wells collagen-coated plates. DMEM/F-12 media supplemented with 3% FBS and 1% P/S was used to seed and incubate cells with 4-PBA (5 mM) and/or TM (2.4 μM) for 48 h. Vehicle-incubated cells were used as control. Afterwards, cells were harvested and washed once with cold PBS 1X. Then, cells were resuspended in Annexin V binding buffer and labeled with 5 μg/ml of FITC Annexin V at room temperature for 15 min. Thereafter, a final concentration of 1 μM of TO-PRO®-3 dye was added and incubated during 15 min on ice. Finally, stained cells were analyzed by flow cytometry in a Guava® easyCyte 8HT Flow Cytometer (Merck Millipore, MA, USA).

On the other hand, activation of caspase-3 and caspase-7 was determined using the *Caspase-Glo® 3/7 assay* (Promega Corporation, WI, USA) according to the manufacturer´s instructions. The luminescence intensity was measured on the PHERAstar luminometer (BMG Labtech, Germany).

Mass spectrometry and proteomic analysis

Proteins were extracted by incubating whole cell extracts (WCEs) of normal and polycystic cholangiocytes (both human and rat treated with 4-PBA or vehicle) in 7 M urea, 2 M thiourea, 4% CHAPS for 30 min at room temperature with shaking. Afterwards, proteins were digested following the Filter-Aided Sample Preparation (FASP) protocol (4) with minor modifications. Trypsin was added to a trypsin:protein ratio of 1:10, and the mixture was incubated overnight at 37ºC, dried out in a RVC2 25 speedvac concentrator (Christ), and resuspended in 0.1% formic acid (FA).

Peptide separation was performed on a nanoElute liquid chromatograph (Bruker) coupled online to a novel hybrid trapped ion mobility spectrometry (TIMS) – quadrupole time of flight (TOF) mass spectrometer (timsTOF Pro) (Bruker) that uses the parallel accumulation – serial fragmentation (PASEF) acquisition method. An aliquot (200 ng) of each sample was directly loaded in a 50ºC heated nanoElute FIFTEEN C18 (75 µm x 150 mm) analytical column (Bruker) and eluted at 400 nl/min with a 30 min linear gradient of 3–50% acetonitrile. Of note, the employed mass spectrometer takes advantage of the novel PASEF scan mode, which multiplies the sequencing speed without any loss in sensitivity,(5) and has been proven to provide outstanding analytical speed and sensibility for proteomics analyses.(6)

Protein´s identification and quantification in each sample were carried out using PEAKS software (Bioinformatics solutions). Searches were carried out against a database consisting of human or rat entries (Uniprot/Swissprot), with precursor and fragment tolerances of 20 ppm and 0.05 Da. Only proteins identified with at least two peptides at false discovery rate (FDR) <1% were considered for further analysis. Protein abundance was calculated by the PEAKSQ module, and quantitative data was loaded onto Perseus platform (7) and further processed (log2 transformation, imputation). In addition, Venn diagrams were created with the *InteractiVenn* online software (http://www.interactivenn.net/),(8) while heatmaps and protein enrichment

analysis were generated using the *Functional Enrichment analysis tool* (FunRich) version 3.1.3 (Funrich Industrial Co. Ltd, Hong Kong).(9)

Functional analyses of proteins were performed using the online STRING (10) (https://string-db.org/) and the DAVID bioinformatics recourses (https://david.ncifcrf.gov/summary.jsp).(11) STRING is a biological database of known and predicted direct (physical) and indirect (functional) protein-protein interactions, displaying protein association networks based on the annotated proteomes maintained by Swiss-Prot.(12, 13) Confidence scores, scaled between zero and one, are provided for each protein-protein interaction, indicating the estimated likelihood that a given interaction is biologically meaningful, specific and reproducible, given the supporting evidence. In turn, the supporting evidence is divided into one or more 'evidence channels' that are delineated by edges of different color, depending on the origin and type of the evidence.(12) Moreover, a functional characterization of a set of proteins can be conducted through enrichment analysis, which are done for a variety of classification systems [Gene Ontology (GO), KEGG, Pfam and InterPro], employing a Fisher's exact test followed by a correction for multiple testing.(12) DAVID is a GO term annotation and enrichment analysis tool used to highlight the most relevant GO terms associated with a given gene list. A Fisher exact test is used in order to determine whether the proportion of genes considered into certain GO term or categories differ significantly between the dataset and the background. Biological process (BP), molecular function (MF) and cellular component (CC) categories were assessed, and only GO terms with an enrichment p-value<0.05 were considered for comparison and discussion.

Results

Expression of UPR-related sensors in normal and cystic cholangiocytes *in vitro* under the presence of ER stress modulators

The incubation of 4-PBA did not have significant common effects on the baseline expression levels of *ATF6* and *PERK* in normal and cystic cholangiocytes *in vitro* (Supporting Fig. 1). In contrast, 4-PBA upregulated the baseline expression of *IRE1α* in both normal and cystic cholangiocytes *in vitro* (Supporting Fig. 1). The presence of TM increased the expression levels of *IRE1α* in both normal and cystic (ADPKD and ADPLD) cholangiocytes, but this effect was not modified with 4-PBA (Supporting Fig. 1).

Expression of pro-fibrotic and pro-inflammatory genes in the liver of wild-type and PCK rats under baseline conditions or after the administration of ER stress regulators

As previously reported,(14, 15) the liver of PCK rats showed increased expression of pro-fibrotic (i.e., *Col1a1*, *α-Sma*, *Ctgf*) and pro-inflammatory genes (i.e., *Il-6* and *Cxcl1*) compared to normal animals (Supporting Fig. 2). Chronic administration of 4-PBA did not modify the levels of pro-fibrotic and pro-inflammatory genes in the liver of PCK rats (Supporting Fig. 2). Of note, chronic administration of TM stimulated the expression of pro-fibrotic (i.e., *Col1a1*, *α-Sma*, *Ctgf*) and pro-inflammatory genes (i.e., *Il-6* and *Cxcl1*) in the liver of PCK rats compared to control PCK rats, which were not significantly affected after 4-PBA treatment (Supporting Fig. 2).

Biochemical and macroscopic features of the experimental animal groups

Similar to patients with ARPKD, the PCK rat undergoes hepato-renal cystogenesis. For this reason, we compared some hepatic and renal biochemical and macroscopic parameters in WT and PCK rats in control conditions, as well as in PCK rats that received 4-PBA, TM, or the combination of both drugs (Supporting Table 3). As previously reported,(14, 15) control PCK rats underwent a markedly enlargement of both kidneys, entailing a significant increased kidney/body weight ratio compared to the WT animals (Supporting Table 3). Likewise, the serum levels of creatinine and urea (i.e., two commonly used indicators of the renal function) were found increased in the PCK animals compared to WT rats (Supporting Table 3). Chronic administration of 4-PBA did not have any effect on the renal disease manifestations of PCK rats. However, the administration of TM to PCK rats significantly reduced all the kidney parameters analyzed [i.e., kidney weight, kidney/body weight, creatinine, UCR (urea/creatinine)] compared to control PCK rats (Supporting Table 3). In this regard, the administration of TM along with 4-PBA counteracts the TM-induced effects (Supporting Table 3). Altogether, these data indicate that fine tuning of ER stress regulates liver and renal cystogenesis. The levels of ER stress in polycystic liver and kidneys, and their role in cystic pathobiology, might be different and dependent of the type of gene found mutated, deserving further investigation.

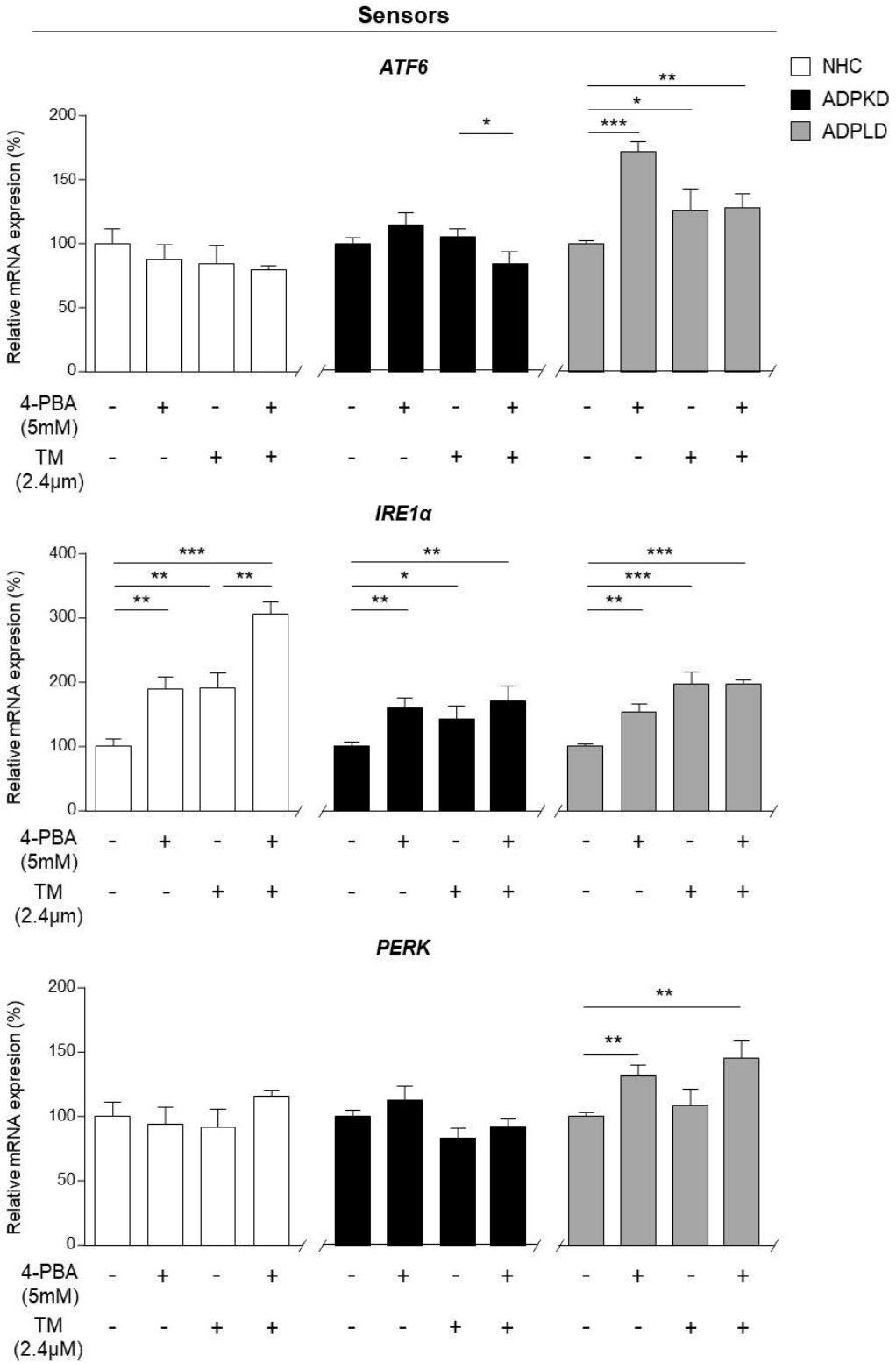

Supporting Fig. 1. Modulation of UPR signaling in cholangiocytes. Transcriptional analysis of the UPR sensors in normal (NHC; n=5) and cystic (ADPKD and ADPLD; n=4-5) cholangiocytes after incubation with 4-PBA, TM or the combination of both ER stress modulators. Parametric unpaired Student's t-test test was used.

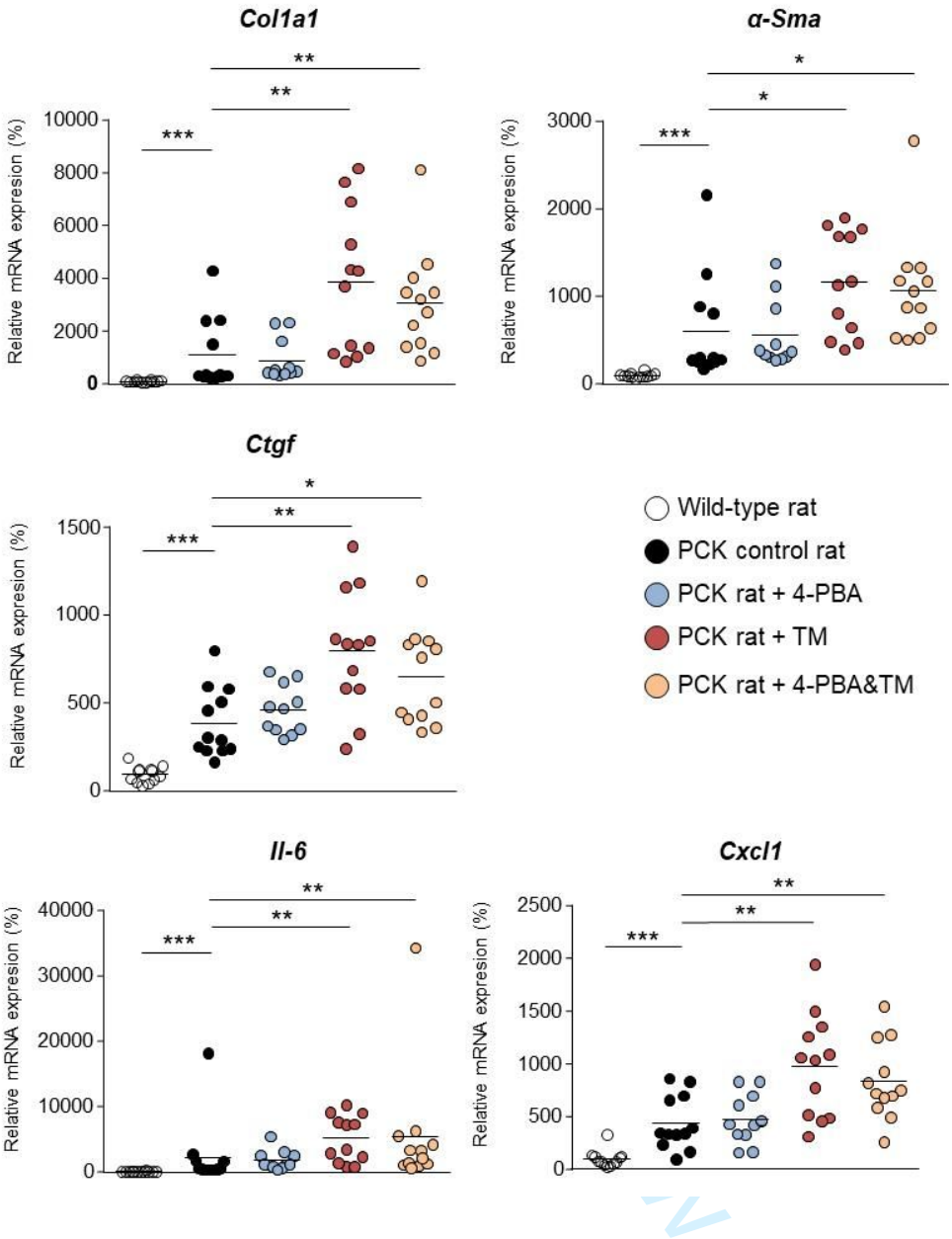

Supporting Fig. 2. Expression of pro-fibrotic and pro-inflammatory genes in liver of wild-type and PCK rats under baseline conditions and/or under the administration of 4-PBA and/or TM. mRNA expression levels of pro-fibrotic (i.e., *Col1a1*, *α-Sma* and *Ctgf*) and pro-inflammatory (i.e., *Il-6* and *Cxcl1*) genes in the liver of wild-type (n=12) and control PCK rats (n=12), as well as in PCK rats chronically treated with 4-PBA (n=12) and/or TM (n=12). Parametric unpaired Student's t-test and Non-parametric Mann-Whitney test were used.

Supporting Table 1. Demographic and clinical features of the study cohort

Variable	PLD (n=16)	Gallbladder (n=14)	Healthy liver (n=14)
Age, mean ± SEM	51.25 ± 3.07	63.36 ± 3.63	66.36 ± 2.02
Age, range	35 - 71	31 - 79	55 - 80
Gender			
Female (%)	14 (87.50)	5 (35.71)	7 (50.00)
Male (%)	2 (12.50)	9 (64.29)	7 (50.00)
Germline mutation			
PRKCSH (%)			
c.1341-2A>G	4 (25.00)	-	-
c.292+1G>C	1 (6.25)	-	-
SEC63 (%)			
1702delGAA	1 (6.25)	-	-
Other (%)	8 (50.00)	-	-
Unknown (%)	2 (12.50)	-	-
Number of cysts (%)			
<10	2 (12.50)	-	-
10-40	5 (31.25)	-	-
>40	8 (50.00)	-	-
Unknown	1 (6.25)	-	-
Biochemistry, mean ± SEM			
ALT (U/L)	39.07 ± 7.80	55.86 ± 12.96	25.29 ± 3.49
AST (U/L)	30.00 ± 4.57	58.50 ± 16.53	26.17 ± 3.06

Supporting Table 2. Primers employed for quantitative PCR (all from Sigma-Aldrich)

	Gene		Sequences
Human primers			
	ATF6	Forward	5'-GCTGGATGAAGTTGTGTCAGAG-3'
		Reverse	5'-GCTTCTCTTCCTTCAGTGGC-3'
	CHOP	Forward	5'-TCTTCATACATCACCACACC-3'
		Reverse	5'-CTTGTGACCTCTGCTGGTTC-3'
	GAPDH	Forward	5'-CCAAGGTCATCCATGACAAC-3'
		Reverse	5'-TGTCATACCAGGAAATGAGC-3'
	GRP78	Forward	5'-GAGCTGTGCAGAAACTCCGGCG-3'
		Reverse	5'-ACCACCTGCTGAATCTTTGGAATTCGAGT-3'
	IRE1α	Forward	5'-AGGGACAGGAGGGAATCGTA-3'
		Reverse	5'-CAGTCCCTAATGCCACACCT-3'
	PERK	Forward	5'-CAGGCAAAGGAAGGAGTCTG-3'
		Reverse	5'-AACAACTCCAAAGCCACCAC-3'
	XBP1	Forward	5'-GCAGGTGCAGGCCCAGTTGTCAC-3'
		Reverse	5'-CCCCACTGACAGAGAAAGGGAGG-3'
Rat primers			
	α-Sma	*Forward*	5'-CGCCATCAGGAACCTCGAGAAG-3'
		Reverse	5'-ATCATCACCAGCAAAGCCCG-3'
	Atf6	Forward	5'-TCTTCAACTCAGCACGTTCC-3'
		Reverse	5'-GCTTCTCTTCCTTCAGTGGC-3'
	Chop	Forward	5'-AGTCATGGCAGCTGAGTCTC-3'
		Reverse	5'-CTGACTGGAATCTGGAGAGC-3'
	Col1a1	*Forward*	5'-GACTGTCCCAACCCCCAAA-3'
		Reverse	5'-CTTGGGTCCCTCGACTCCTA-3'
	Ctgf	*Forward*	5'-CTAGCTGCCTACCGACTGGA-3'
		Reverse	5'-GCCCATCCCACAGGTCTTAG-3'
	Cxcl1 (*Il-8* homolog)	*Forward*	5'-ACTCAAGAATGGTCGCGAGG-3'
		Reverse	5'-ACGCCATCGGTGCAATCTAT-3'
	Gapdh	Forward	5'-TGTGAACGGATTTGGCCGTA-3'
		Reverse	5'-ATGAAGGGGTCGTTGATGG-3'
	Grp78	Forward	5'-GAGCTGTGCAGAAACTCCGGCG-3'
		Reverse	5'-ACCACCTGCTGAATCTTTGGAATTCGAGT-3'
	Il-6	*Forward*	5'-CATTCTGTCTCGAGCCCACC-3'
		Reverse	5'-AGTCCCAAGAAGGCAACTGG-3'
	Ire1α	Forward	5'-GACTATGCAGCCTCACTTCC-3'
		Reverse	5'-CAAGACATCCCCAGATTCAC-3'
	Perk	Forward	5'-TTTCACTGTGGAGTCCCTTC-3'
		Reverse	5'-CTGGTACTCCCATTCTAGGC -3'
	Xbp1	Forward	5'-GCAGGTGCAGGCCCAGTTGTCAC-3'
		Reverse	5'-CCCCACTGACAGAGAAAGGGAGG-3'

Supporting Table 3. Biochemical and macroscopical determinations in wild-type and PCK rats

Parameters	A	B	C	D	E					
	Wild-type rats	PCK rats (non – treated)	PCK rats (4-PBA – treated)	PCK rats (TM – treated)	PCK rats (4-PBA&TM – treated)	*p* value (A *vs* B)	*p* value (B *vs* C)	*p* value (B *vs* D)	*p* value (B vs E)	*p* value (D *vs* E)
Body weight (g)	627.92 ± 13.81	626.96 ± 11.39	521.68 ± 15.58	549.63 ± 7.54	460.21 ± 22.62	0.8291	< 0.0001	< 0.0001	< 0.0001	0.0011
Liver/body weight (%)	3.01 ± 0.07	5.93 ± 0.75	5.20 ± 0.60	7.81 ± 0.70	6.89 ± 0.73	<0.0001	0.1643	0.0204	0.0915	0.3724
Bile flow (µl/min/g)	0.022 ± 0.0021	0.026 ± 0.0070	0.026 ± 0.0052	0.041 ± 0.0088	0.070 ± 0.020	0.9526	0.8198	0.1764	0.0708	0.4432
Alkaline phosphatase (U/L)	96.67 ± 6.98	209.33 ± 18.45	234.18 ± 22.12	323.00 ± 18.00	314.00 ± 18.17	<0.0001	0.2663	0.0006	0.0013	0.7283
Aspartate aminotransferase (U/L)	201.33 ± 25.81	228.33 ± 23.02	252.36 ± 16.68	381.67 ± 21.97	460.00 ± 45.35	0.4433	0.2664	<0.0001	<0.0001	0.1778
Alanine aminotransferase (U/L)	61.00 ± 4.52	47.33 ± 1.54	63.64 ± 4.05	62.67 ± 3.86	82.33 ± 6.54	0.0090	0.0009	0.0013	<0.0001	0.0167
De Ritis ratio (AST/ALT)	3.28 ± 0.31	4.98 ± 0.63	4.18 ± 0.46	6.41 ± 0.60	6.29 ± 0.99	0.0377	0.2032	0.0252	0.1066	0.3098
Albumin (g/L)	9.25 ± 0.24	5.84 ± 0.29	6.61 ± 0.37	7.04 ± 0.48	7.29 ± 0.60	<0.0001	0.0759	0.0433	0.0405	0.7444
Protein total (g/dL)	6.23 ± 0.12	5.71 ± 0.19	5.84 ± 0.07	6.14 ± 0.15	5.90 ± 0.16	0.0317	0.1640	0.0343	0.2977	0.2821
Kidney weight (g)	1.58 ± 0.04	3.94 ± 0.32	3.88 ± 0.20	2.41 ± 0.11	3.18 ± 0.11	<0.0001	0.5969	<0.0001	0.0165	<0.0001
Kidney/body weight (%)	0.51 ± 0.01	1.25 ± 0.09	1.52 ± 0.13	0.876 ± 0.04	1.39 ± 0.14	<0.0001	0.0454	0.0001	0.1822	0.0008
Blood urea (mg/dL)	35.00 ± 0.87	55.00 ± 5.59	44.36 ± 2.77	32.67 ± 2.64	40.67 ± 3.07	<0.0001	0.2038[a]	<0.0001	0.0221	0.0070
Creatinine (mg/dL)	0.48 ± 0.02	0.69 ± 0.03	0.62 ± 0.02	0.53 ± 0.02	0.51 ± 0.02	<0.0001	0.1051	0.0002	0.0001	0.5700
UCR (Urea/Creatinine)	74.64 ± 4.24	78.01 ± 5.18	71.67 ± 3.88	61.47 ± 3.61	80.37 ± 6.68	0.6233	0.3450	0.0045	0.7828	0.0103

Abbrev: 4-PBA, 4-phenylbutyric acid sodium salt; AST, aspartate aminotransferase; ALT, alanine aminotransferase; TM, tunicamycin; VS, versus.

References

1. Han X, Zhang X, Li H, Huang S, Zhang S, Wang F, et al. Tunicamycin enhances the antitumor activity of trastuzumab on breast cancer in vitro and in vivo. Oncotarget. 2015;6(36):38912-25.
2. Urribarri AD, Munoz-Garrido P, Perugorria MJ, Erice O, Merino-Azpitarte M, Arbelaiz A, et al. Inhibition of metalloprotease hyperactivity in cystic cholangiocytes halts the development of polycystic liver diseases. Gut. 2014;63(10):1658-67.
3. Erice O, Labiano I, Arbelaiz A, Santos-Laso A, Munoz-Garrido P, Jimenez-Aguero R, et al. Differential effects of FXR or TGR5 activation in cholangiocarcinoma progression. Biochim Biophys Acta Mol Basis Dis. 2018;1864(4 Pt B):1335-44.
4. Wisniewski JR, Zougman A, Mann M. Combination of FASP and StageTip-based fractionation allows in-depth analysis of the hippocampal membrane proteome. J Proteome Res. 2009;8(12):5674-8.
5. Meier F, Brunner AD, Koch S, Koch H, Lubeck M, Krause M, et al. Online Parallel Accumulation-Serial Fragmentation (PASEF) with a Novel Trapped Ion Mobility Mass Spectrometer. Mol Cell Proteomics : MCP. 2018;17(12):2534-45.
6. Meier F, Beck S, Grassl N, Lubeck M, Park MA, Raether O, et al. Parallel Accumulation-Serial Fragmentation (PASEF): Multiplying Sequencing Speed and Sensitivity by Synchronized Scans in a Trapped Ion Mobility Device. J Proteome Res. 2015;14(12):5378-87.
7. Tyanova S, Cox J. Perseus: A Bioinformatics Platform for Integrative Analysis of Proteomics Data in Cancer Research. Methods Mol Biol. 2018;1711:133-48.
8. Heberle H, Meirelles GV, da Silva FR, Telles GP, Minghim R. InteractiVenn: a web-based tool for the analysis of sets through Venn diagrams. BMC bioinformatics. 2015;16:169.
9. Pathan M, Keerthikumar S, Chisanga D, Alessandro R, Ang CS, Askenase P, et al. A novel community driven software for functional enrichment analysis of extracellular vesicles data. J Extracell Vesicles. 2017;6(1):1321455.
10. Szklarczyk D, Gable AL, Lyon D, Junge A, Wyder S, Huerta-Cepas J, et al. STRING v11: protein-protein association networks with increased coverage, supporting functional discovery in genome-wide experimental datasets. Nucleic Acids Res. 2019;47(D1):D607-D13.
11. Huang DW SB, Lempicki RA. Systematic and integrative analysis of large gene lists using DAVID bioinformatics resources. Nat Protoc. 2009;4(1):14.
12. Szklarczyk D, Morris JH, Cook H, Kuhn M, Wyder S, Simonovic M, et al. The STRING database in 2017: quality-controlled protein-protein association networks, made broadly accessible. Nucleic Acids Res. 2017;45(D1):D362-D8.
13. von Mering C, Huynen M, Jaeggi D, Schmidt S, Bork P, Snel B. STRING: a database of predicted functional associations between proteins. Nucleic Acids Res. 2003;31(1):258-61.
14. Mason SB, Liang Y, Sinders RM, Miller CA, Eggleston-Gulyas T, Crisler-Roberts R, et al. Disease stage characterization of hepatorenal fibrocystic pathology in the PCK rat model of ARPKD. Anat Rec. 2010;293(8):1279-88.
15. Masyuk TV, Huang BQ, Masyuk AI, Ritman EL, Torres VE, Wang X, et al. Biliary dysgenesis in the PCK rat, an orthologous model of autosomal recessive polycystic kidney disease. Am J Pathol. 2004;165(5):1719-30.